Supplementary file for Manuscript :

Designed synthesis of CO_2 promoted copper(II) coordination polymers: synthesis, structural, spectroscopic characterization and versatile functional property studies†

Pritam Ghosh,[a] Additi Roychowdhury,[ab] Montserrat Corbella,[c] Asim Bhaumik,[d] Partha Mitra,[d] Shaikh M. Mobin,[e] Ayan Mukherjee,[f] Soumen Basu,[f] and Priyabrata Banerjee*[ab]

Content	**Page**

Table S1 Selected bond distances (Å) and angles (°) for $[Cu(bpy)(C_2O_4)]_n$ (**1**)

Selected bond distance(Å)		Selected bond angles (°)	
Cu(1)-N(1)	1.994(3)	O(1)-Cu(1)-O(2)	90.31(10)
Cu(1)-N(2)	2.005(3)	O(1)-Cu(1)-O(3)	90.13(10)
Cu(1)-O(1)	1.980(3)	O(1)-Cu(1)-O(4)	77.79(10)
Cu(1)-O(2)	1.987(2)	O(1)-Cu(1)-N(1)	173.65(11)
Cu(1)-O(3)	2.309(3)	O(2)-Cu(1)-N(2)	175.78(11)
Cu(1)-O(4)	2.313(3)	O(1)-Cu(1)-N(2)	93.86(10)
C(12)-O(1)	1.265(4)	O(4)-Cu(1)-N(2)	94.42(10)
C(12_a)-O(4)	1.228(4)	N(1)-Cu(1)-N(2)	80.93(11)
C(12)-C(12_a)	1.569(5)	O(3)-Cu(1)-N(2)	103.16(10)
C(5)-C(6)	1.484(5)		
C(6)-C(7)	1.382(5)		
C(7)-C(8)	1.374(6)		
C(8)-C(9)	1.372(5)		
C(9)-C(10)	1.366(5)		
C(10)-N(2)	1.346(5)		
N(2)-C(6)	1.345(4)		
N(1)-C(5)	1.347(4)		

Table S2 Selected bond distances (Å) and angles (°) for ligand (**L[1]**)

Selected bond distance(Å)			
C(6)-C(7)	1.527(3)	C(2)-C(3)	1.369(3)
C(7)-C(12)	1.380(3)	C(3)-C(4)	1.367(4)
C(12)-C(11)	1.387(3)	C(4)-C(5)	1.358(3)
C(11)-C(10)	1.368(3)	C(5)-N(1)	1.338(3)
C(10)-C(9)	1.385(3)	N(1)-C(1)	1.333(2)
C(9)-C(8)	1.379(3)	C(6)-N(3)	1.452(3)
C(8)-C(7)	1.385(3)	N(3)-C(13)	1.367(3)
C(6)-N(2)	1.440(3)	C(13)-C(14)	1.394(3)
N(2)-C(1)	1.375(2)	C(17)-N(4)	1.336(3)
C(1)-C(2)	1.391(3)	N(4)-C(13)	1.345(2)
Selected bond angles (°)			
N(2) -C(6)-C(7)	109.24(13)	N(2)-C(6)-N(3)	110.68(14)
N(3) -C(6)-C(7)	114.06(13)	C(1) -N(1)-C(5)	117.58(15)
C(1) -N(2)-C(6)	123.55(14)	C(13)-N(4)-C(17)	117.36(16)
C(6)-N(3)-C(13)	123.97(15)		

Table S3 Selected bond distances (Å) and angles (°) for $[Cu(2\text{-}AMP)_2(C_2O_4)]_n$ (**2**)

Selected bond distances (Å)		Selected bond angles (°)	
Cu(1)-N(1)	2.0323(19)	O(1) -Cu(1) -O(2)	76.08(5)
Cu(1)-N(1_a)	2.0323(19)	O(1) -Cu(1) -N(1)	89.44(7)
Cu(1)-O(2)	2.3805(15)	O(1) -Cu(1) -O(1_a)	87.01(6)
Cu(1)-O(2_a)	2.3805(15)	O(1) -Cu(1) -O(2_a)	85.79(5)
Cu(1)-O(1_a)	1.9930(15)	O(1) -Cu(1) -N(1_a)	176.30(7)
Cu(1)-O(1)	1.9930(15)	O(2) -Cu(1) -N(1)	92.37(6)
N(1)-C(1)	1.348(4)	O(1_a) -Cu(1) -O(2)	85.79(5)
C(1)-C(2)	1.355(4)	O(2) -Cu(1) -O(2_a)	155.00(6)
C(2)-C(3)	1.388(4)	O(2) -Cu(1) -N(1_a)	104.68(6)
C(3)-C(4)	1.347(4)	O(1_a) -Cu(1) -N(1)	176.30(7)
C(4)-C(5)	1.405(3)	O(2_a) -Cu(1) -N(1)	104.68(6)
C(5)-N(1)	1.345(3)	N(1) -Cu(1) -N(1_a)	94.14(7)
C(5)-N(2)	1.339(3)	O(1_a)-Cu(1)-O(2_a)	76.08(5)
O(1) -C(6)	1.254(2)	O(1_a) -Cu(1)-N(1_a)	89.44(7)
O(2) -C(6_b)	1.241(3)	O(2_a) -Cu(1) -N(1_a)	92.37(6)
C(6) -C(6_b)	1.568(3)		

Table S4 Selected bond distances (Å) and angles (°) for $[Cu(L^2)(Cl)]$ (**3**)

Selected bond distances (Å)			
Cu(1)-N(3)	2.007(7)	N(1)-C(5)	1.309(10)
Cu(1)-N(1)	2.005(6)	C(2)-C(3)	1.373(15)
Cu(1)-N(2)	2.075(6)	C(15)-C(20)	1.394(11)
Cu(1)-O(1)	2.344(5)	N(2)-C(7)	1.468(10)
Cu(1)-Cl(1)	2.255(2)	C(3)-C(4)	1.368(14)
O(1)-C(20)	1.377(10)	N(2)-C(14)	1.497(9)
N(1)-C(1)	1.348(11)	C(16)-C(17)	1.381(14)
C(1)-C(2)	1.373 (12)	C(17)-C(18)	1.348(16)
N(2)-C(6)	1.512(10)	C(18)-C(19)	1.403(15)
N(3)-C(13)	1.340(12)	C(19)-C(20)	1.350(13)
N(3)-C(9)	1.335(11)		
Selected bond angles (°)			
Cl(1)-Cu(1)-O(1)	95.43(15)	N(3)-Cu(1)-O(1)	92.1(3)
Cl(1)-Cu(1)-N(1)	93.18(19)	N(1)-Cu(1)-N(3)	170.1(3)
Cl(1)-Cu(1)-N(2)	174.37(18)	Cl(1)-Cu(1)-N(3)	92.0(2)
N(1)-Cu(1)-N(2)	82.0(2)	N(3)-Cu(1)-N(2)	92.3(3)
N(2)-Cu(1)-O(1)	88.0(2)	N(1)-Cu(1)-O(1)	95.8(2)

Table S5 Crystallographic details of **1**, **1'**, **2**, **3** and **L**[1]

	1	1'	2	3	L^1
Empirical Formula	$C_{12}H_8CuN_2O_4$, $2(H_2O)$	$C_{46}H_{38}CuN_2P_2,ClO_4$	$C_{12}H_{12}CuN_4O_4$	$C_{20}H_{20}ClCuN_3O$	$C_{17}H_{16}N_4$
M	343.79	843.72	339.81	417.39	276.34
Crystal system	Triclinic	Monoclinic	Monoclinic	Monoclinic	Monoclinic
Space group	P-1(No. 2)	P 21/n(No. 14)	C2/c (No. 15)	C2/c (No. 15)	C2/c (No. 15)
a(Å)	8.9254(18)	10.1166(10)	13.4876(14)	22.477(4)	8.887(8)
b(Å)	9.0881(18)	14.9515(14)	11.2653(12)	12.052(2)	17.728(15)
c(Å)	9.652(2)	26.557(3)	8.7010(9)	20.103(4)	18.635(16)
α (deg)	110.363(4)	90	90	90	90
β (deg)	97.535(4)	91.743(2)	93.755(2)	102.013(5)	90.707(12)
γ (deg)	105.761(4)	90	90	90	90
V($Å^3$)	684.0(2)	4015.1(7)	1319.2(2)	5326.5(17)	2936(4)
Z	2	4	4	8	8
T(K)	293	150	293	293	293
λ (Mo Kα)	0.71073	0.71073	0.71073	0.71073	0.71073
Dc (g cm^{-3})	1.669	1.396	1.711	1.041	1.250
μ (mm^{-1})	1.626	0.737	1.678	0.930	0.077
Total data	6459	29280	6866	15481	10933
Unique Reflection	2417	6423	1171	4042	2813
Rint	0.028	0.056	0.024	0.064	0.032

Table S6 CHN analysis of **1**, **1'**, **2**, **3**, **4**, **L**[1] and **L**[2]

Compound	C,H,N Analysis
1	Anal. Calcd for $C_{12}H_{12}N_2O_6Cu$: C, 41.88% ; H, 3.49% ; N, 8.14%. Found: C, 42. 05%; H, 3.36%; N,8.04%.
1'	Anal. Calcd for $C_{46}H_{38}CuN_2P_2,ClO_4$: C, 65.42% ; H, 4.50% ; N, 3.31%. Found: C, 65.37%; H, 4.43%; N,3.41%.
2	Anal. Calcd for $C_{12}H_{12}N_4O_4Cu$: C, 42.38%; H, 3.53%, N, 16.48 %. Found: C, 42.28% ; H, 3.48%, N, 16.42% .
3	Anal. Calcd. for $C_{20}H_{20}N_3OCuCl.(7H_2O)$:C, 44.16% ; H, 6.25% ; N, 7.73%. Found: C, 43.97%; H, 5.97%; N, 7.62%.
4	Anal. Calcd for $C_{34}H_{34}N_7O_4Cu_2Cl_2$: C, 51.06% ; H, 4.25% ; N, 12.26%. Found: C, 50.95%; H, 4.30%; N, 12.39%.
L[1]	Anal. Calcd for $C_{17}H_{16}N_4$: C, 73.82% ; H, 5.78% ; N, 20.26 %. Found: C, 73.91%; H, 5.9%; N, 20.17%.
L[2]	Anal. Calcd for $C_{20}H_{21}N_3O$: C, 75.23%; H, 6.58%; N, 13.16%. Found: C, 75.25%; H, 6.59%; N, 13.17%.

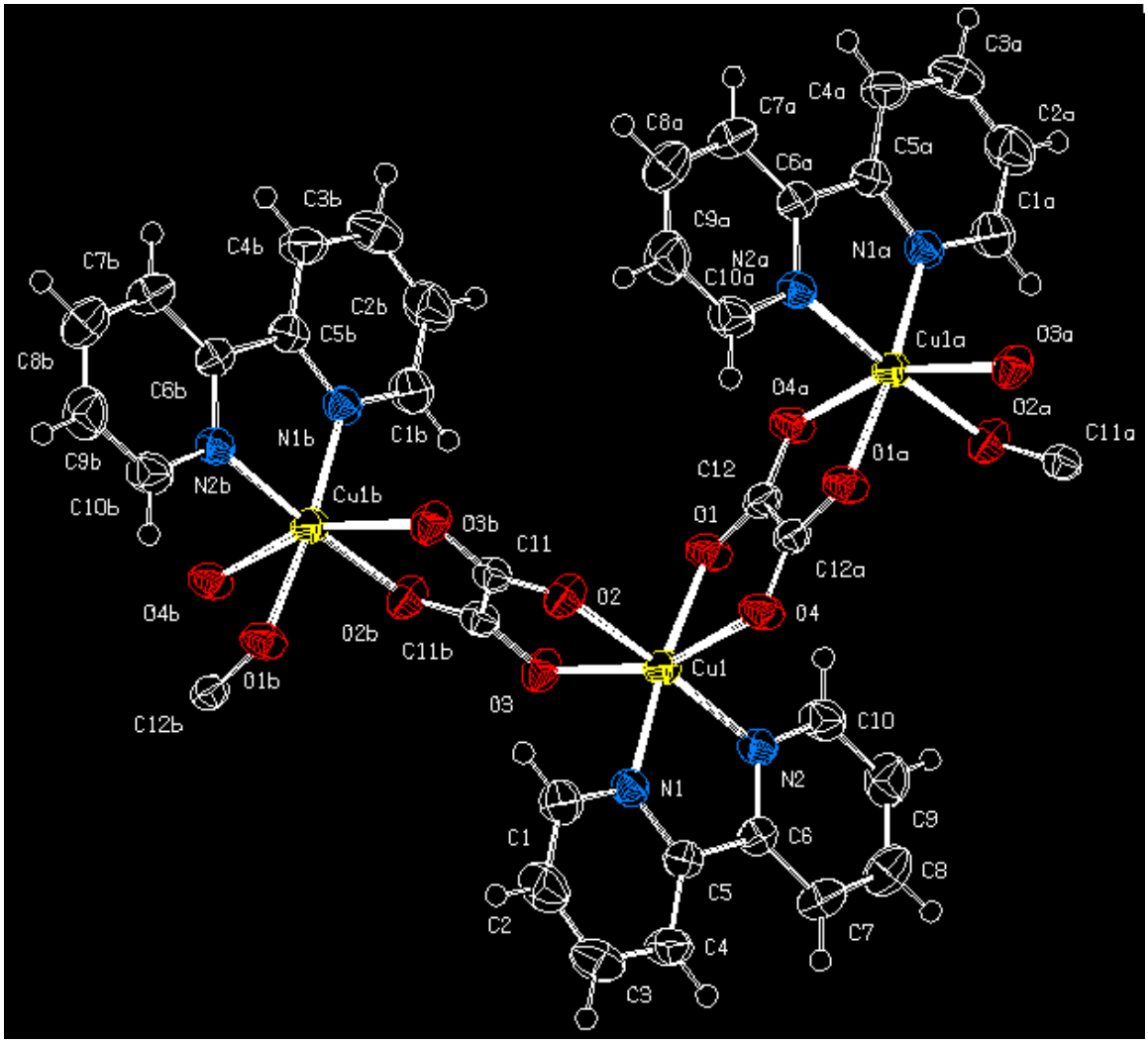

Fig. S1 ORTEP of complex **1**.

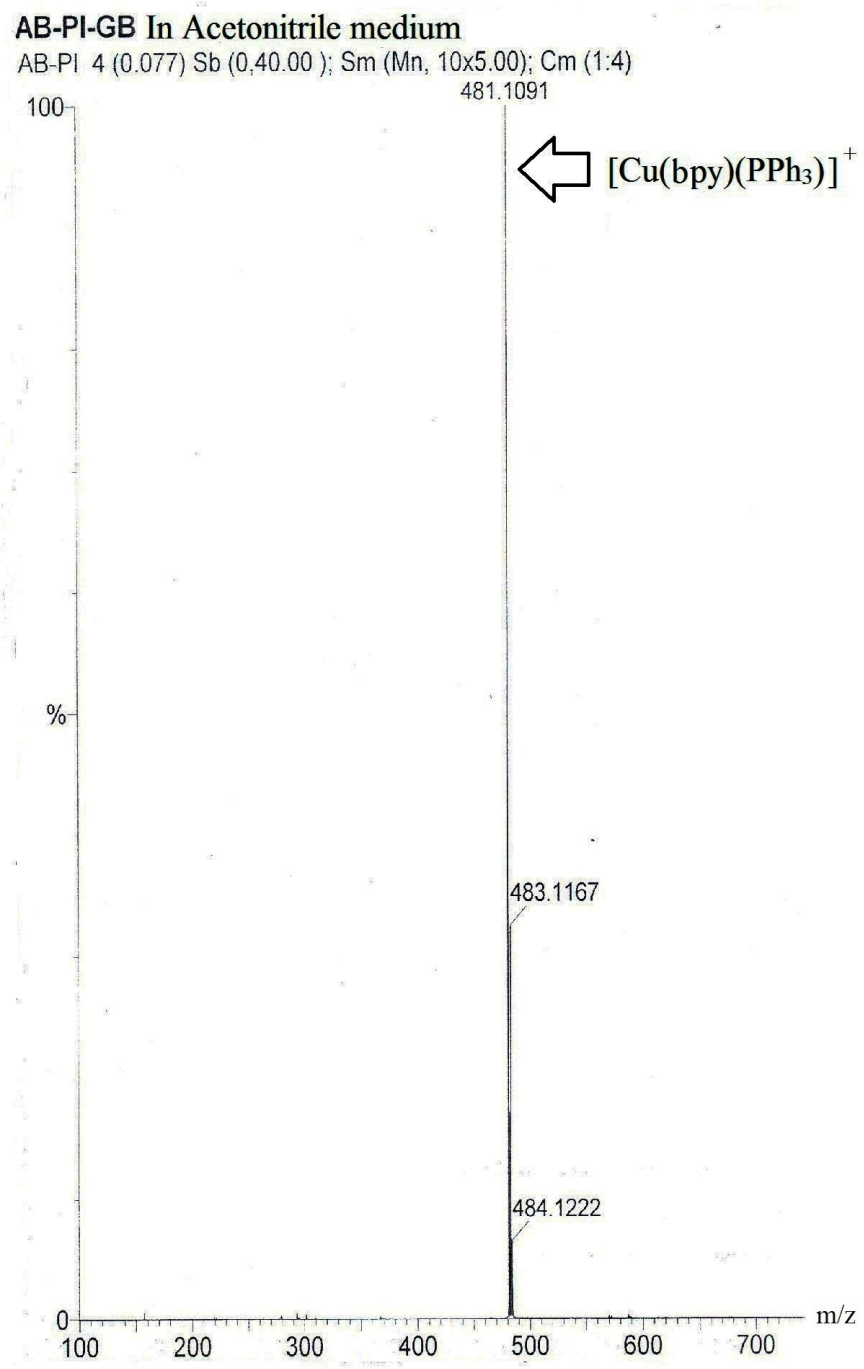

Fig. S2 ESI-MS spectrum of **1′** in acetonitrile.

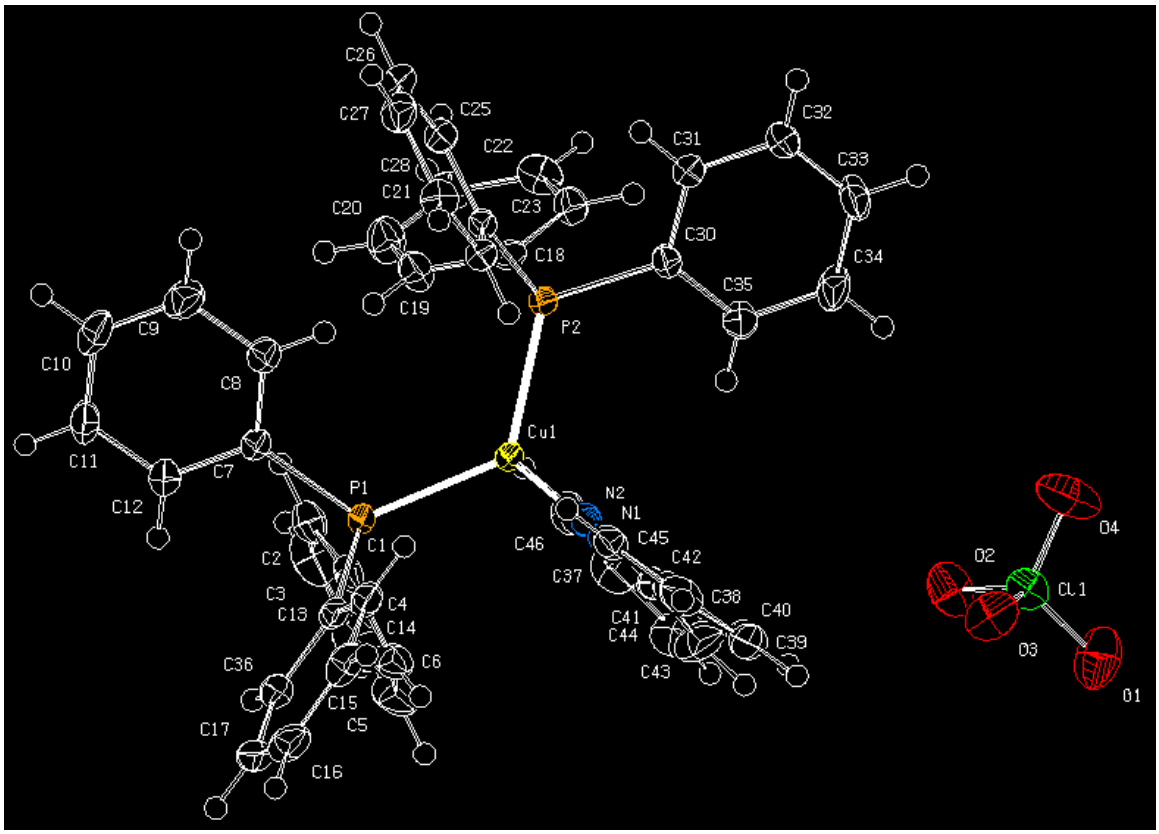

Fig. S3 ORTEP diagram of **1′**.

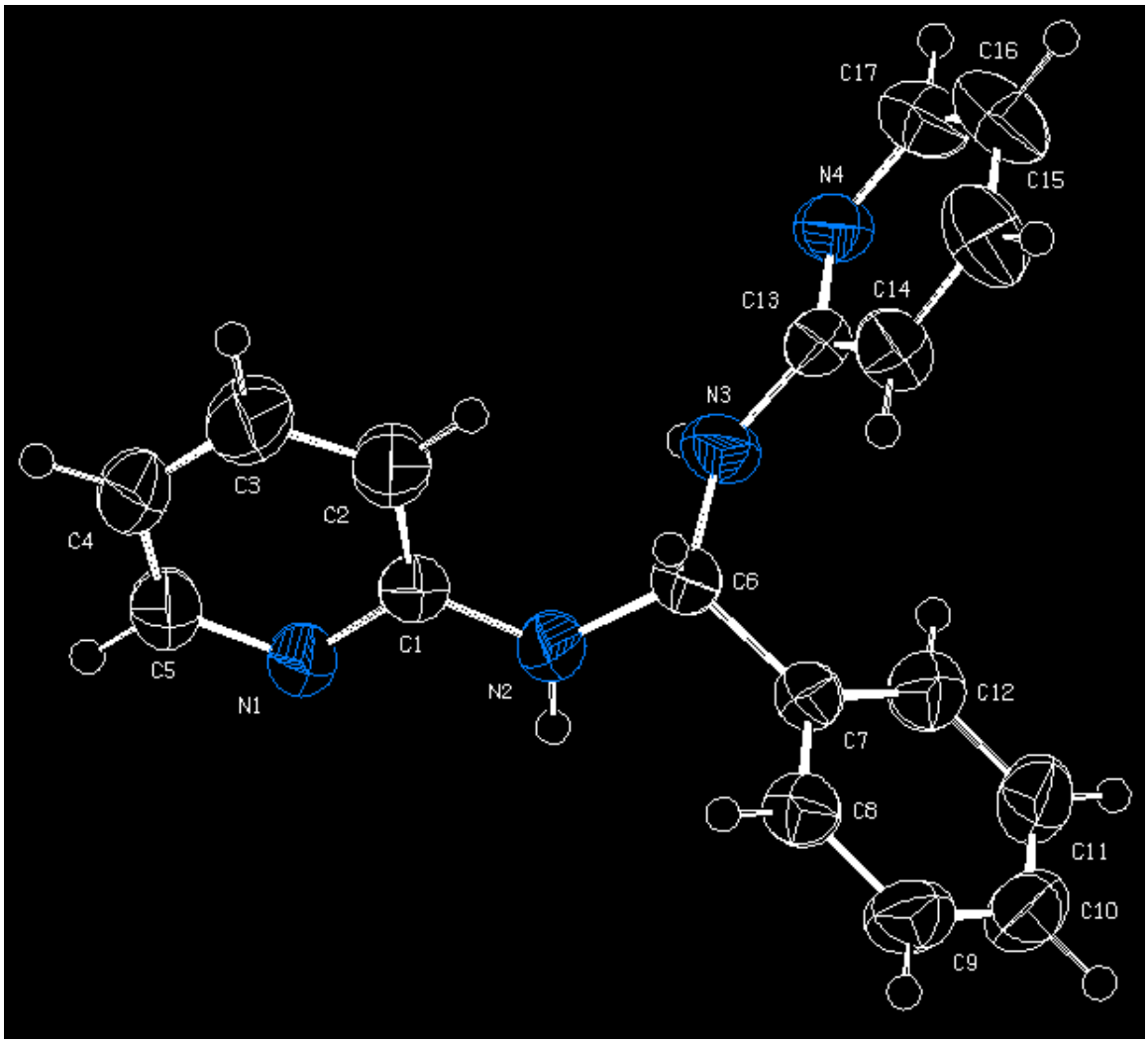

Fig. S4 ORTEP of ligand **L**[1].

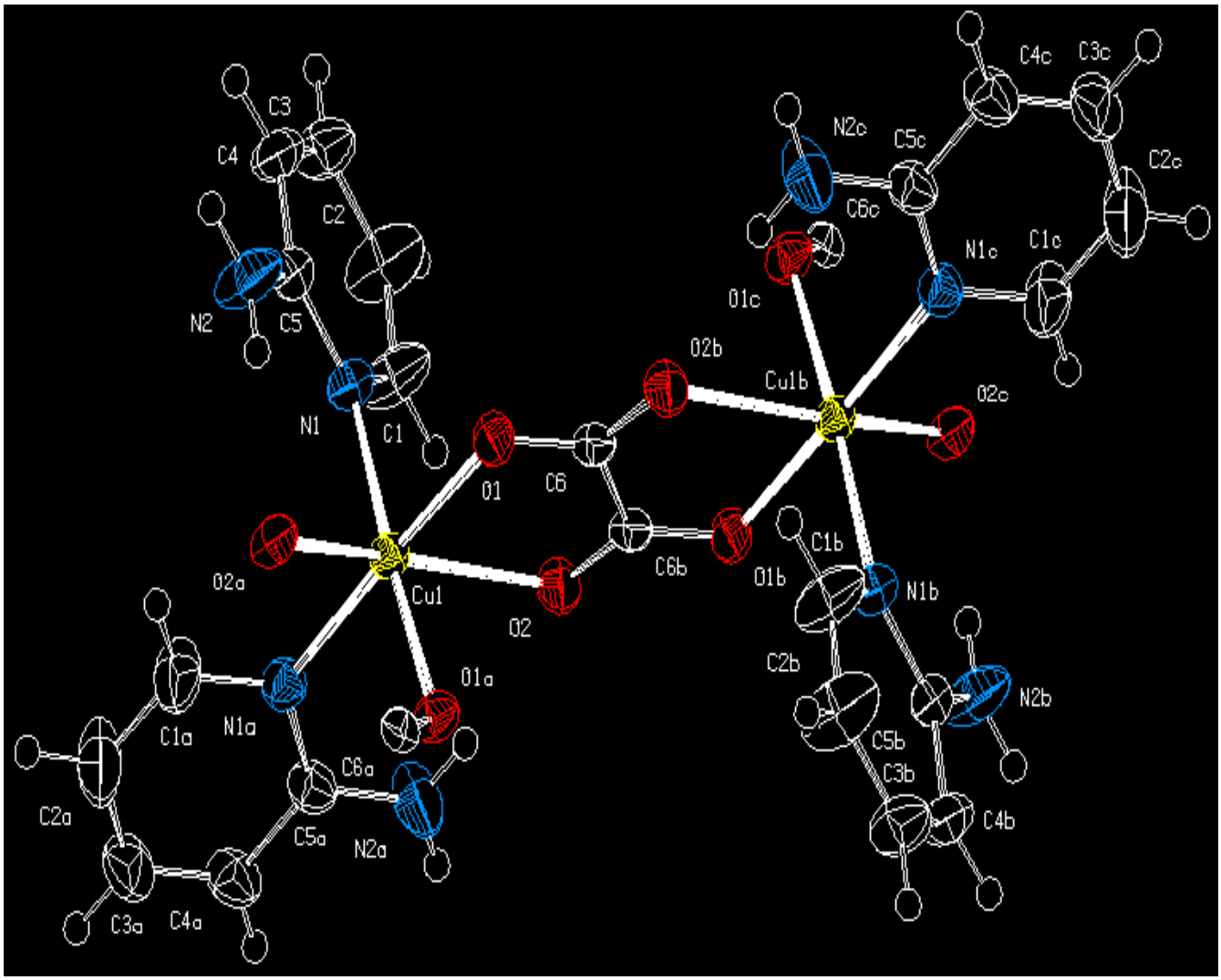

Fig. S5 ORTEP of complex **2**.

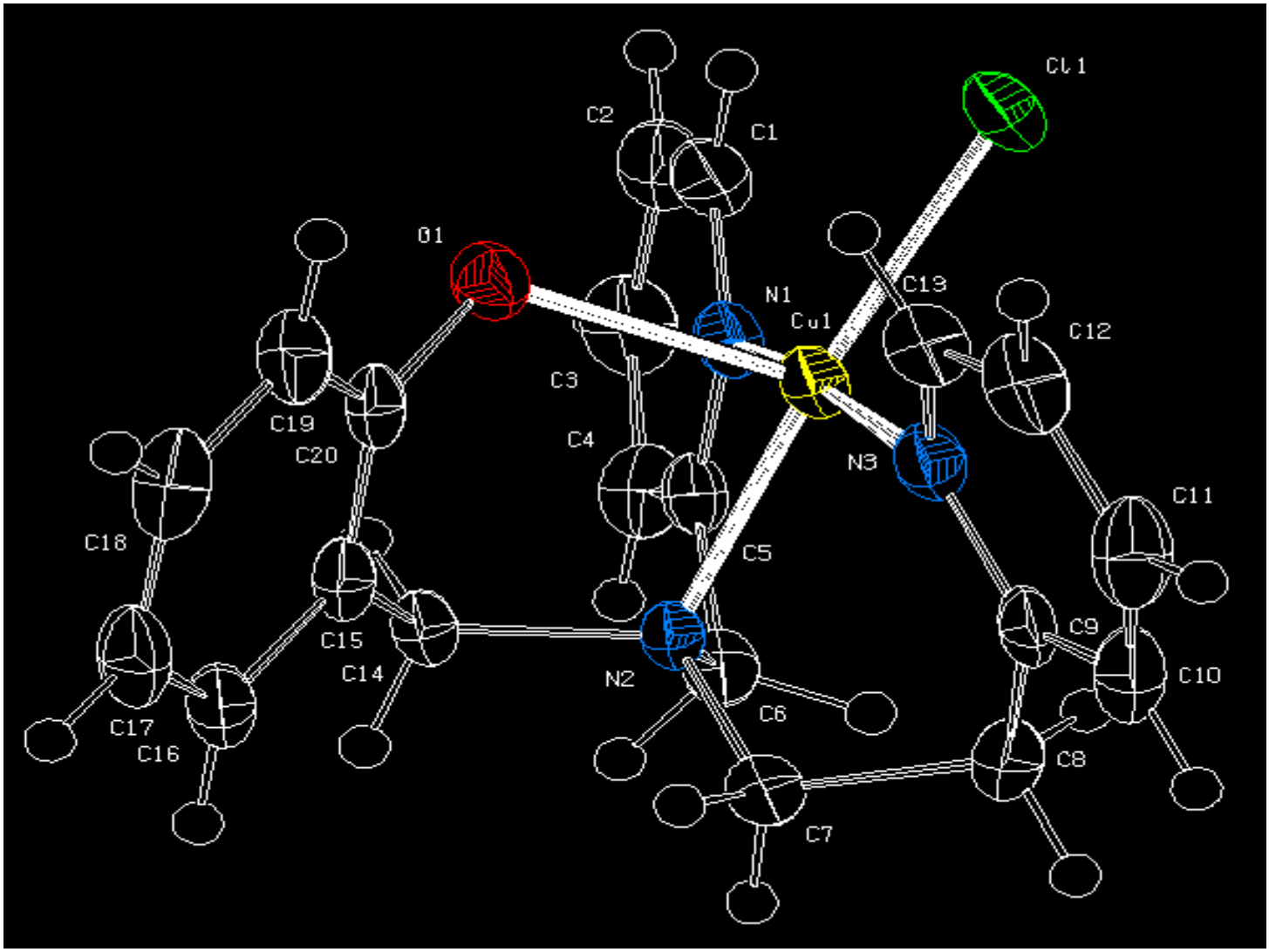

Fig. S6a ORTEP of complex **3**.

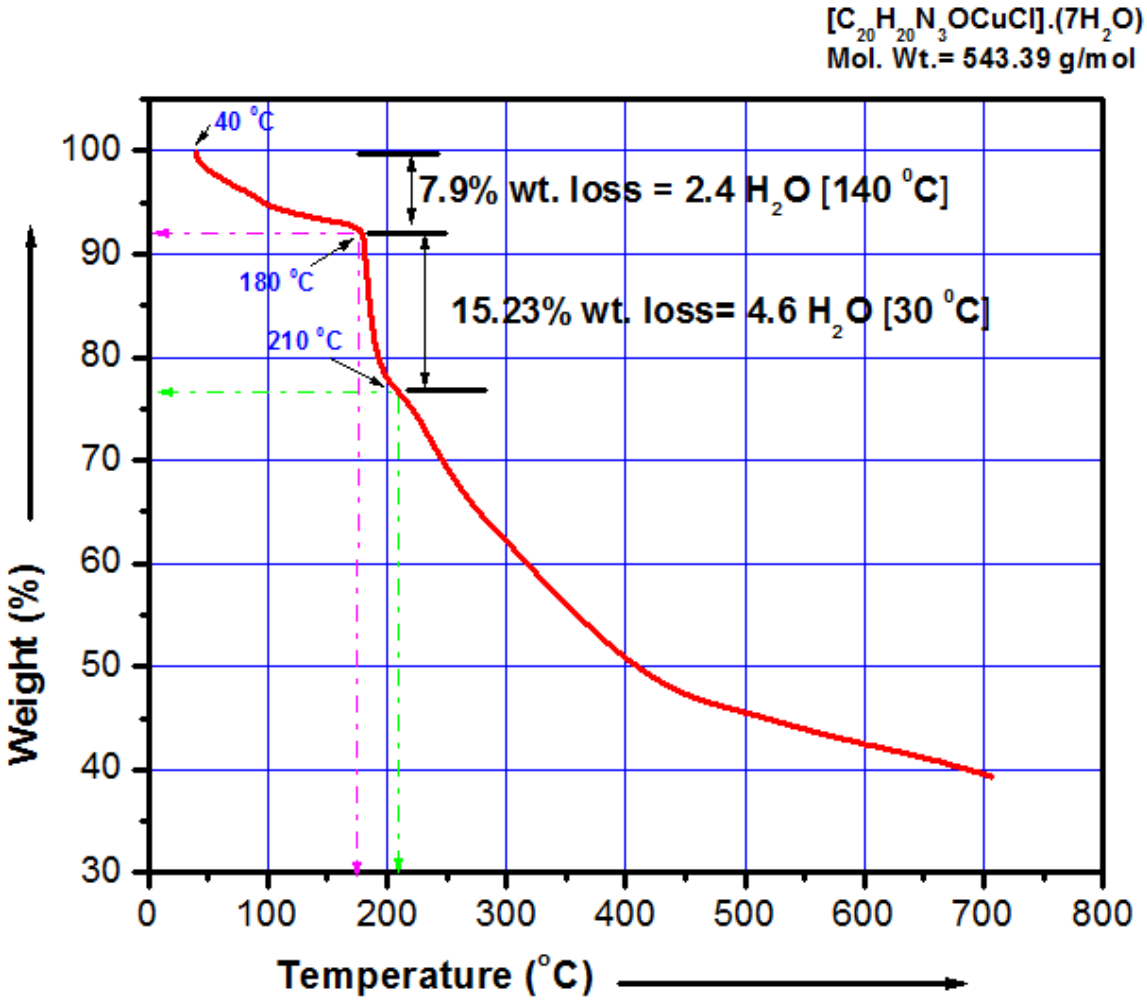

Fig. S6b TGA profile of complex **[Cu(L²)(Cl)]·7H₂O.**

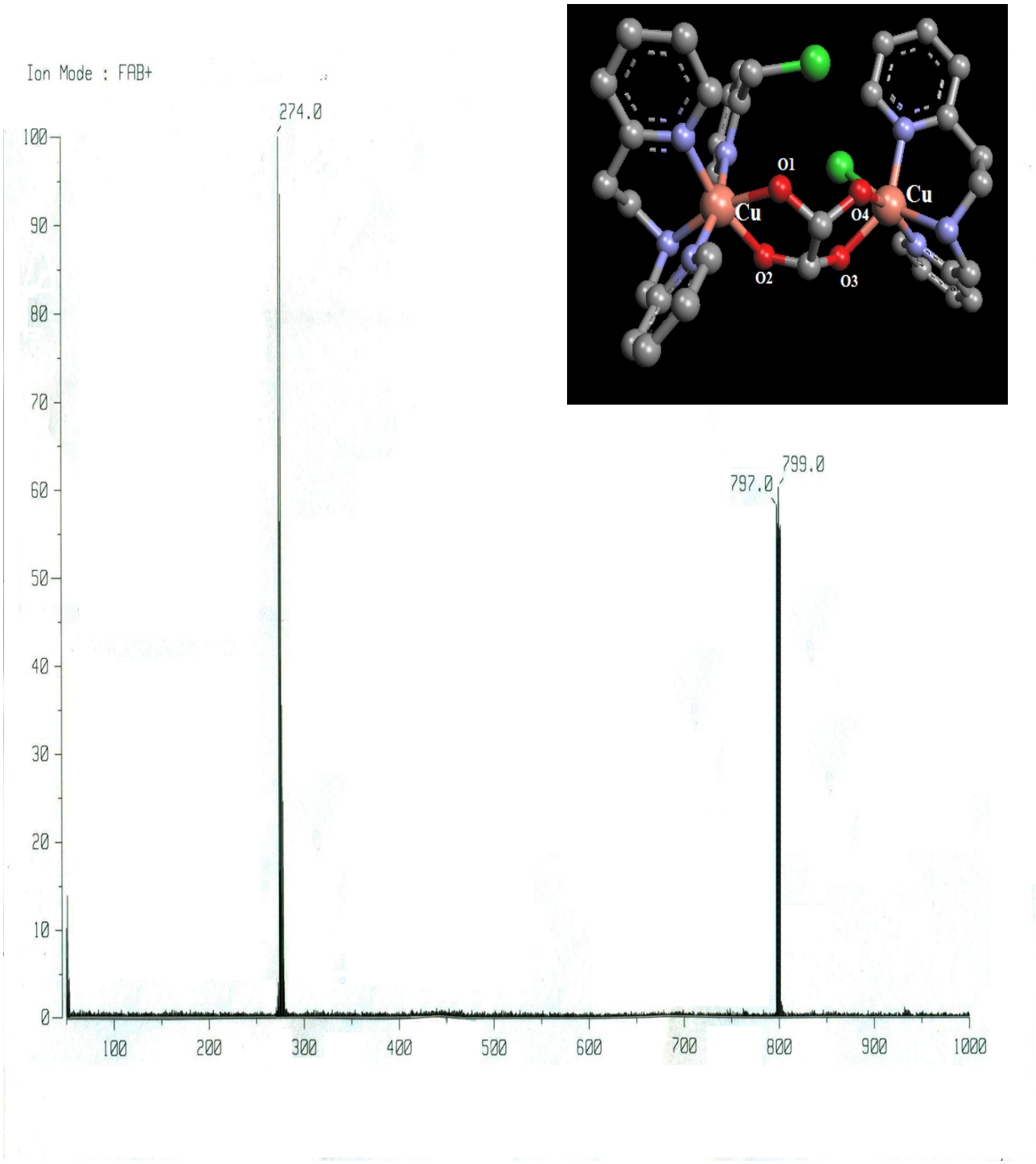

Fig. S7 FAB-MS spectrum of **4** (Inset: proposed molecular view of **4**).

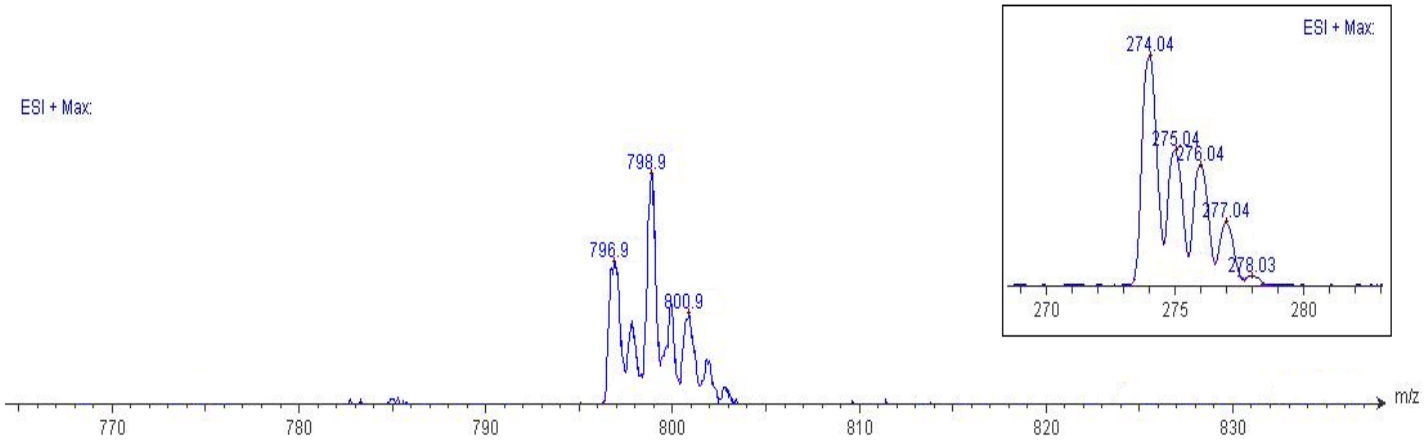

Fig. S8 ESI-MS spectrum of **4** (Inset: fragmented part at m/z~274).

IR frequencies of $[Cu(bpy)(C_2O_4)]_n$ (**1**).

Characteristic IR Peaks (KBr disk, υ, cm^{-1}): 1652(s), 1089(br), 1447(s) , 773(s), 730(s), 626(s).

Fig. S9 IR spectrum of $[Cu(2\text{-}AMP)_2(C_2O_4)]_n$ (**2**).

Characteristic IR Peaks (KBr disk, υ, cm^{-1}): 1664 (s), 1632 (s), 1594 (s), 1566 (s), 1497 (s), 1452 (s), 1311 (s), 1263 (s), 1167 (s), 796 (s), 763 (s).

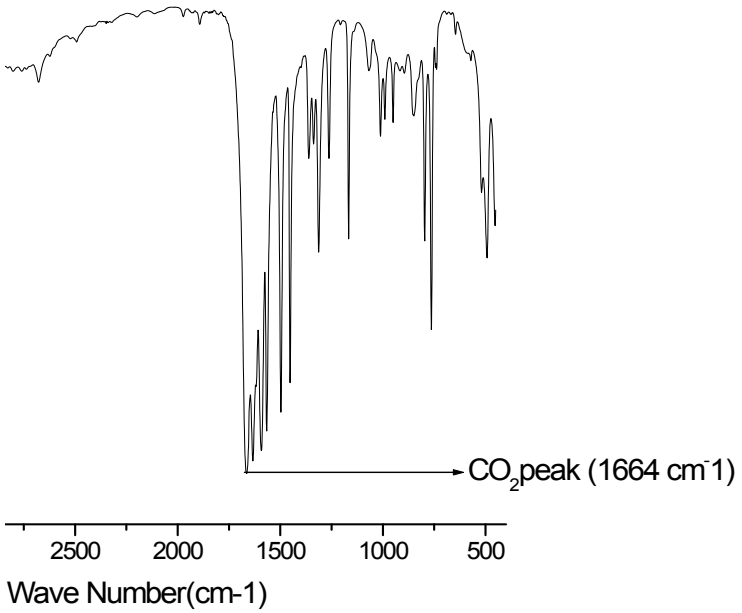

Fig. S10 IR spectrum of [Cu(L^2)(Cl)] (**3**).
Characteristic IR Peaks (KBr disk, υ, cm^{-1}) :
1609 (s), 1484 (s) , 1450 (s) , 1110 (s), 1031 (s), 767 (s).

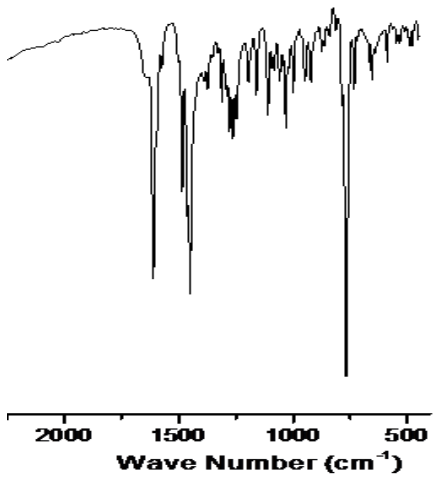

IR frequencies of **4**.
Characteristic IR Peaks (KBr disk, υ, cm^{-1}) : 1633 (s) , 1609 (s) , 1451 (s) , 1157 (s) , 1021 (s) , 763 (s).

Fig. S11 IR spectrum of **1'**.
Characteristic IR Peaks (KBr disk, υ, cm^{-1}) : 488 (s), 514 (s), 622 (s), 695 (s), 747 (s), 1092 (s), 1437 (s), 1480 (s), 1593 (s); of which the peaks 1437, 1028 and 695 are bands coming due to PPh_3.

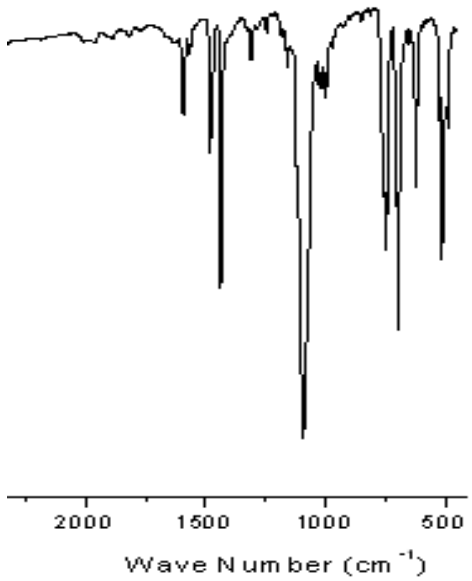

UV-Vis spectroscopic studies
Room temperature UV-Visible

spectral studies of ultrasonicated complex **1** in DMF-MeOH (1:9) have shown that there are peaks at about 215, 245(sh) and 300 nm respectively (Fig. S12a, Table S7). Inset shows the absorption peak at about 700nm [assigned as d-d transition][ref1]. UV-Vis spectral studies of complex **2** in DMF solvent (after 10 minutes of ultrasonication) shows the characteristic peaks at 280,310 nm (Fig. S12b). We are unable to perform higher concentration UV-Visible study with this sample due to its low solubility and rapid degradation. The peaks (<300 nm) are assigned mostly as $\pi \rightarrow \pi^*$ electron transitions of pyridine N atoms and aromatic rings. The absorption peaks at 300 nm may be treated as $n \rightarrow \pi^*$ electronic transition of pyridine N atoms to C_2O_4oxygen atoms. Complex **3** is showing absorption peaks at 215, 260 and 600 nm (Fig. S12c). A structured absorption band (Fig. S12c inset) at 600 nm may be best described as laportte forbidden d_{xz},$d_{xy} \rightarrow d_z^2$ transitions (very weak transition). Complex **4** shows charecteristic absorption peaks at 205,260 nm and 600 nm(inset) (Fig. S12d). The similar broad absorption band like **3** of very very low intensity is appeared at ~ 600 nm for complex **4**, can be attributed as laportte forbidden d_{xz},$d_{xy} \rightarrow d_z^2$ transitions (Table S7).[ref2]

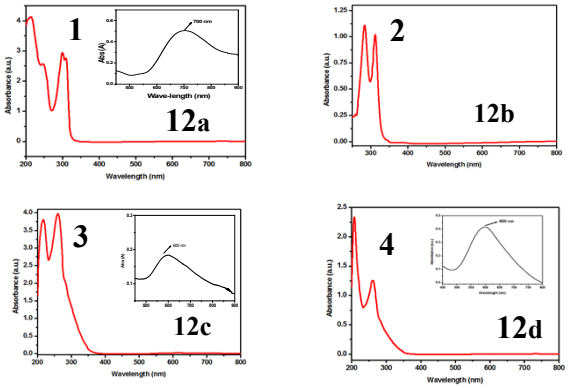

UV-Vis spectrum, **Fig. S12a** Complex **1** in DMF-MeOH and **Fig. S12b** Complex **2** in DMF (after sonication for 10 mins) **Fig. S12c** Complex **3** in MeOH solvent and **Fig. S12d** Complex **4** in DMF-MeOH solvent.

Ref 1: K. D. Karlin, B. I. Cohen, J. C. Hayes, A. Farooq and J. Zubieta, *Inorg. Chem.* 1987**, 26***,* 147.

Ref 2a: A.A. Holder,P. Taylor, A.R. Magnusen, E.T. Moffett,K. Meyer, Y. Hong, S.E. Ramsdale,M. Gordon, J.Stubbs,L.A. Seymour, D. Acharya, R.T. Weber, P.F. Smith, G. C. Dismukes, P. Ji, L. Menocal, F. Bai, J.L. Williams,D.M. Cropek and W.L. Jarrett, *Dalton Trans.*, 2013, **42**, 11881. Ref 2b: M-L Fu, D. Fenske, B. Weinert and O. Fuhr, *Eur. J. Inorg. Chem.*, 2010, 1098-1102.

Table S7 UV-Vis data analysis of Complex **1**, **1'**, **2**, **3**, **4**, $\mathbf{L^1}$ and $\mathbf{L^2}$

Compound	UV-Visible data (λ_{max}/cm^{-1})
1	215, 245(sh), 300, 700
1'	240, 400
2	280, 310
3	215, 260, 600
4	205, 260, 600
L^1	220(sh), 250, 290
L^2	210, 260, 320